Supplementary Materials

Catalytic methane decomposition process on carbon-based catalyst under contactless induction heating

Lai Truong-Phuoc[1], Ahmed Essyed[1], Xuan-Huynh Pham[1], Thierry Romero[1], Jean-Pierre Dath[2], Jean-Mario Nhut[1], Arnaud Brazier[3,*], Loïc Vidal[4], Lam Nguyen-Dinh[5], Cuong Pham-Huu[1,*]

[1]Institute of Chemistry and Processes for Energy, Environment and Health (ICPEES), ECPM, UMR 7515 CNRS, University of Strasbourg, Strasbourg Cedex 02 67087, France.
[2]TotalEnergies One Tech Belgium, Industrial Zone Feluy C, Seneffe B-7181, Belgium.
[3]Hydrogen Business Unit, TotalEnergies Jean Fégier Scientific and Technique Center in Pau, Pau Cedex 64018, France.
[4]The Mulhouse Institute of Materials Science (IS2M), UMR 7361, CNRS, University of Haute-Alsace, Mulhouse 68057, France.
[5]University of Science and Technology, The University of Da-Nang, Da-Nang 550000, Vietnam.

[*]**Correspondence to:** Arnaud Brazier, Hydrogen Business Unit, TotalEnergies Jean Fégier Scientific and Technique Center in Pau, EB429, Avenue Larribau, Pau Cedex 64018, France. E-mail: arnaud.brazier@totalenergies.com; Dr. Cuong Pham-Huu, Institute of Chemistry and Processes for Energy, Environment and Health (ICPEES), ECPM, UMR 7515 CNRS, University of Strasbourg, 25 rue Becquerel, Strasbourg Cedex 02 67087, France. E-mail: cuong.pham-huu@unistra.fr

1 | Characterization techniques

Scanning electron microscopy (SEM) was performed on a Tescan VEGA III and ZEISS 2600F microscope. The sample was deposited onto a sample holder by a conductive graphite tape to avoid any loading effect problems.
Transmission electron microscopy (TEM) was performed on a JEOL ARM-200F operating at an accelerated voltage of 200 kV, equipped with a probe corrector for spherical aberrations and a point-to-point resolution of 80 pm. Elemental mapping was finally performed by scanning transmission electron microscopy (STEM) on a JEOL ARM-200F electron microscope equipped with a Gatan energy filter and a cold field emission (FEG) gun operating at 200 kV with a grating resolution of 1.5 Å. For these measurements, the samples were dispersed by ultrasonic treatment (5 min) in chloroform solution and a drop of each suspension was deposited on a copper grid covered with a holey carbon membrane for observation.
X-ray tomography (CT) was performed on an X-Ray Solution tomograph, model Easytom 150–160 (RX solution SAS, Chavanod, France) on the ICS tomography platform (UPR 22, CNRS, Strasbourg, France). The X-ray generator is an open-tube Hamatsu microfocus with tungsten filament and tungsten target. The detector is a Varian PaxScan 2520DX1920x1536 pixel flat panel sensor (pixel size 1/4.127 µ m x 127 µm) – 16 bits. The scan is carried out with the following parameters: Resolution = 1.2 µm, Source – sampling distance = 3.29 mm, Source – sensor 1/4,347 mm, X-ray energy = 80 kV, beam intensity = 65 µ A. The 1984 projections are made on 360°. Average = 15 images per position. The sensor has a frame rate of 2 frames per second. The entire scan lasts 4.5 hours. The reconstruction method used is filtered rear-projection.
Thermogravimetric analysis (TGA) was performed on a thermogravimetric (TG) analyzer (Thermo) using a temperature program between 30 and 1000 °C at a heating rate of 10 °C/min, under air with a flow of 60 mL/min. For the analysis a weight of 20 mg of the sample was deposited inside a platinum crucible suspended inside the ceramic tube localized inside the TGA setup.
Raman spectroscopy analysis was conducted on an ARAMIS Horiba LabRAM Raman spectrometer. The spectra were acquired in the range 500 - 4000 cm^{-1} at the laser excitation wavelength of 532 nm.

2 | Gas chromatography (GC) analysis

Gas fraction analysis (on-line)
Two GC were used in order to enable the separation and analysis in continuous mode of hydrocarbon produced during the reaction.

GC1: Analysis of permanent gas (H_2, N_2, O_2, CH_4, CO) (module A) and of carbon dioxide and light hydrocarbon products (CO_2, C_1-C_4) (module B). The detailed description of the different modules is summarized in the different tables below.

GC1	SRA Instrument model R3000 µ-GC	
Module A	Carrier gas	Argon Constant pressure: 25 psi (1.7 bar)
	Column	MS5A 10 m (+ Backflush) + Poraplot U 3 m T = 75°C
	Detector	µ-TCD
Module B	Carrier gas	Helium Constant pressure: 21.0 psi (1.4 bar)
	Column	Poraplot U 8 m T = 60°C
	Detector	µ-TCD

GC2: Analysis of gaseous hydrocarbon products

Instrument	Varian CP 3800
Sampling	Air actuated sample 6 ports valve T = 200°C
Injector	T = 220 °C (split of 50/1)
Carrier gas	Helium (constant pressure: 8.0 psi, 0.5 bar)
Column	CP Sil-5-CB Length: 60m, ID: 0.53 mm, OD: 1.5 mm
Detector	FID at 250 °C
Temperature program	70°C (5 min) 250°C (ramping rate of 15 °C/min) holding time 5 min

Liquid fraction analysis (off-line)
The GC analytical solution enables the separation and analysis of hydrocarbon products condensed during the reaction, in particular the analysis of C6-C30 hydrocarbons

Instrument	Varian CP 3800
Sampling	0.5 µL (liquid)
Injector	T = 200°C (split 50/1)
Carrier gas	Helium, constant pressure (5.0 psi, 0.3 bar)
Column	RTX®-1
Detector	FID at 250 °C
Temperature program	50 °C (4 min) 260°C (ramping rate of 10 °C/min) holding time 120 min.

3 | Supplementary Figure 1. Hydrogen selectivity on MESOC+_R0 and R1

The selectivity of hydrogen and other hydrocarbon products, i.e. C2 fraction, determined on the MESOC+ catalyst (first and second cycles noted R0 and R1) is presented in Fig. S1. The hydrogen selectivity is accounted for about 90 ± 10 % at low reaction temperature, i.e. 700 °C and 750 °C, while at higher reaction temperature, i.e. 800 °C, the hydrogen selectivity steadily increases, approaching almost 90 %, after an activation period during which the methane conversion significantly rise from few percent to about 60 %. The low hydrogen selectivity calculated during the activation period at 800 °C could be attributed to the change of the C_2 fraction during the activation period, which makes the quantitative calculation of hydrogen selectivity more erratic. The other products (not reported) are mostly C_2 fraction (0.5 to 1 %) while the aromatic contribution remains low at about 0.1 %. At the steady-state the hydrogen selectivity is significantly improved as all the reaction products are stabilize making the analysis more accurate.
In the second cycling test under IH (noted R1) the hydrogen selectivity increases to almost 95% which is due to the slight improvement of the methane conversion and also to the reduction of both C_2 and aromatic compounds in the exit stream. Indeed, at high methane conversion the hydrogen GC surface area of the different reaction products is much improved and thus, making the calculation of the selectivity more accurate.

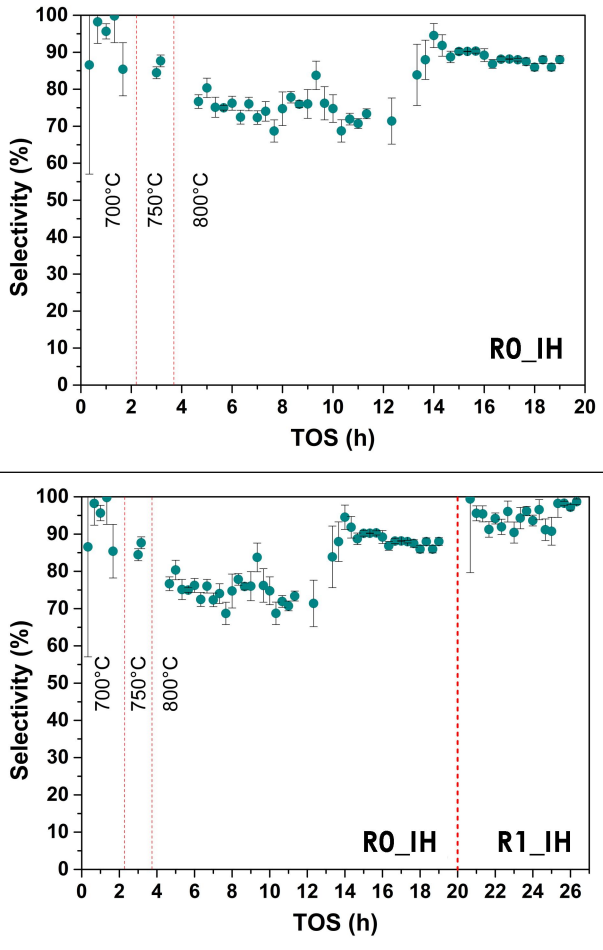

Supplementary Figure 1. | (Top) Selectivity of hydrogen on the MESOC+ (after the first cycle, noted R0) and (Bottom) MESOC+ (after the first and second cycling tests, noted R0 and R1) catalysts operated under IH.

4 | Supplementary Figure 2. Hydrogen selectivity on MESOC+_R0'

The selectivity of hydrogen and other hydrocarbon products, i.e. C2 fraction, determined on the MESOC+ catalyst (first cycle under JH mode, noted R0') is presented in Fig. S2. It is worthy to note that the hydrogen selectivity remains extremely scattered which could be attributed to the relatively low activity, expressed in terms of methane conversion (≤ 10 %), which could induce large error in the calculated value.

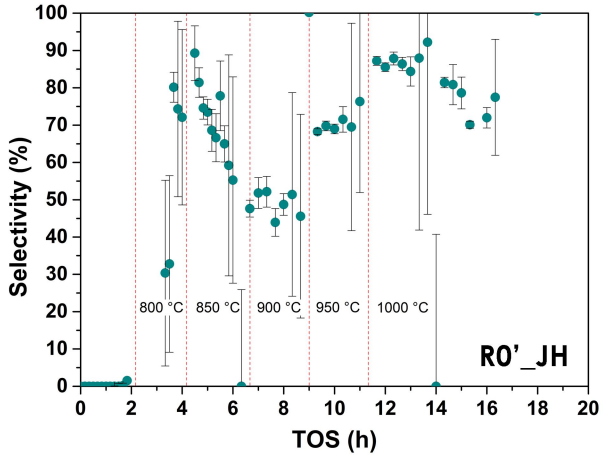

Supplementary Figure 2. | Selectivity of hydrogen on the MESOC+ (R0') catalyst operated under indirect JH with methane conversion not exceeding 15 %.

5 | Supplementary Figure 3. Hydrogen selectivity on MESOC+_R1'

The selectivity of hydrogen and other hydrocarbon products, i.e. C_2 fraction, determined on the MESOC+ catalyst (first cycle under IH (noted R1) followed by a second cycle under JH, noted R1') is presented in Fig. S3. It is worthy to note that the hydrogen selectivity remains extremely scattered (± 200 %) and is attributed to the very low activity, expressed in terms of methane conversion (≤ 1 %), which could induce large error to the calculated value, i.e. low response of the hydrogen and other reaction products surface area in the GC analysis, low flow rate change, error on the calculation of the reactant conversion. Such extremely low activity is attributed to the low specific surface area of the spent catalyst after the first CMD test under IH as generally, the CMD performance on carbon-based catalysts is directly linked with the specific surface area of this later while it is not the case for IH.

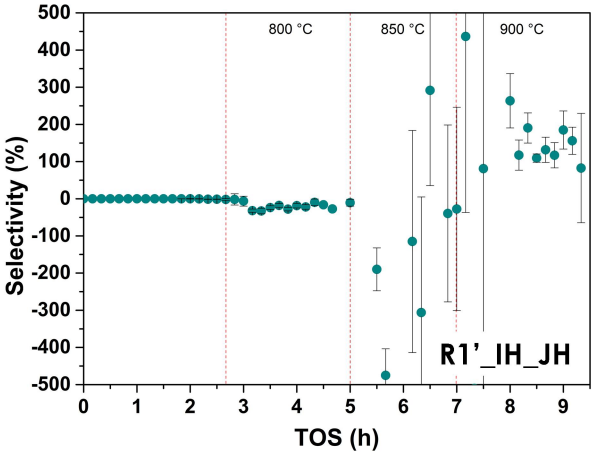

Supplementary Figure 3. | Selectivity of hydrogen and other hydrocarbons on the MESOC+ (first cycle under IH followed by a second cycle under JH, noted R1') catalyst operated under IH.

6 | Supplementary Table 1. Composition of natural gas

The composition of the natural gas from Europe is summarized in Table S1. It is worthy to note that such composition could vary from one source to another, i.e. European vs other countries, especially for CO_2 which can fluctuate on a large range depending to the point of extraction.

Supplementary Table 1. | Composition of natural gas (mol.%)	
Helium	0.09
Nitrogen	1.26
Methane	90.6
Ethane	6.08
Propane	1.19
Iso-Butane	0.28
n-Butane	0.47
CO2	0.004
H2S	0.001